# Chemically and Thermally Ultra-Stable Ba(II) Coordination Polymer with Dual Fluorescence Sensing and High Proton Conductivity

Yue Shu [a,c†], Baoyi Li [b†], Xuxing Chen[c,*],Chenrui Wang[a,b], and Rong Li[a,c,*]

[a]*Hubei Key Laboratory of Micro-Nanoelectronic Materials and Devices, School of Intelligent and manufacturing, Hubei University, Wuhan 430062, P. R. China*

[b]*Fujian Institute of Research on the Structure of Matter, Chinese Academy of Sciences, Fuzhou 350002, P. R. China*

[c]*School of Materials Science & Engineering, Hubei University, Wuhan 430062, P. R. China*

Corresponding authors: cxx0613@hubu.edu.cn (Xu-xing Chen), rli@hubu.edu.cn (Rong Li)

† These authors contributed equally.

## Experimental section

All of the chemicals were purchased from commercial sources and were used without further purification. Metal ion salt $BaBr_2$ (99%) was purchased from Shanghai Aladdin Bio-Chem Technology Co., Ltd. 3,5-bis(3',5'-dicarboxyphenyl)-1H-1,2,4-triazole (97%) was from Jinan Henghua Technology Co., Ltd.

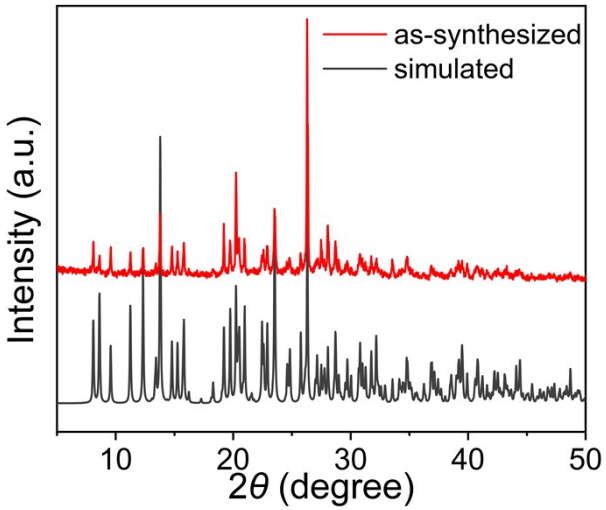


**Figure S1.** PXRD patterns of simulated and as-synthesized of **1**.

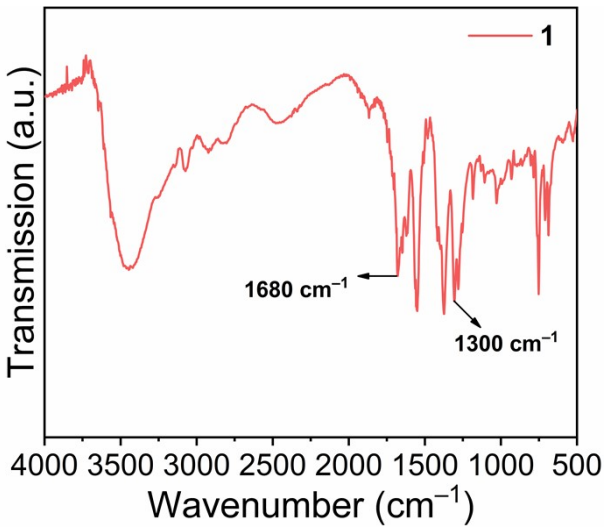


**Figure S2.** FT-IR spectrum for **1**.

† These authors contributed equally.

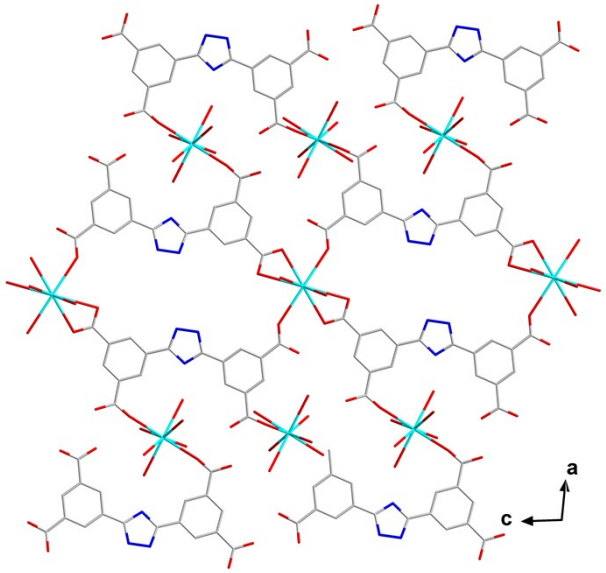


**Figure S3.** Two-dimensional coordination network of compound **1**.

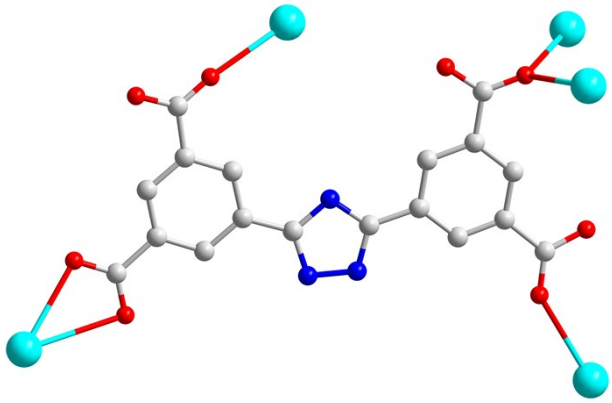

**Figure S4.** $H_2L^{2-}$ coordination mode diagram.

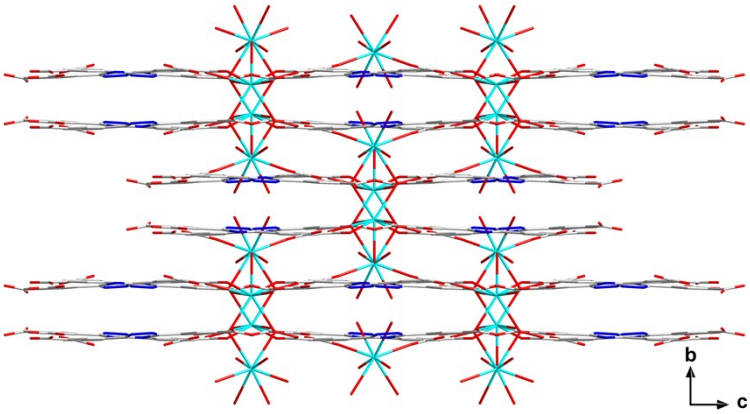


**Figure S5.** The π–π stacking interactions in the framework **1**.

† These authors contributed equally.

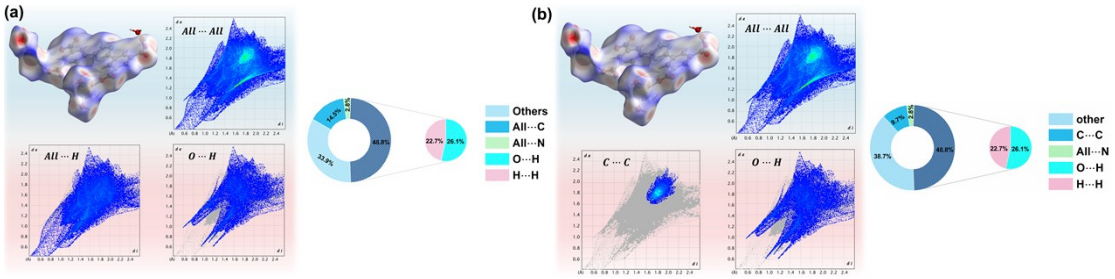


**Figure S6.** Hirshfeld surface analysis and 2D fingerprint plot of weak intermolecular interactions (a) highlighting O–H···O and O–H···N interactions, (b) π–π stacking interactions.

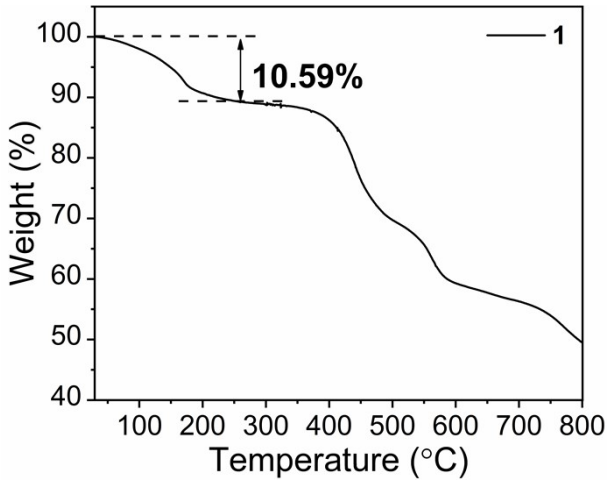


**Figure S7.** TGA curves for compound **1**, the inset is the curve between 30–80 °C.

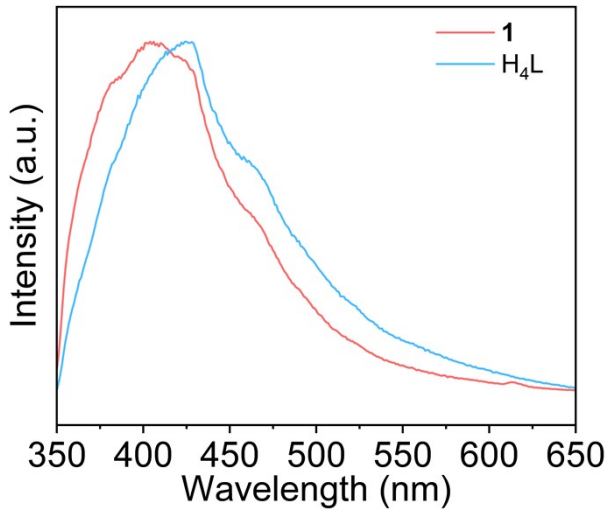


**Figure S8.** The solid-state emission spectrum of $H_4L$ and **1** at room temperature.

† These authors contributed equally.

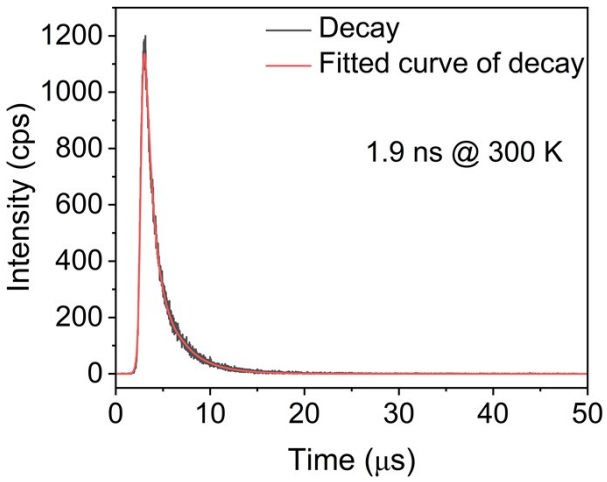


**Figure S9.** Decay lifetime plot of **1** ($\lambda_{ex}$ = 350 nm)

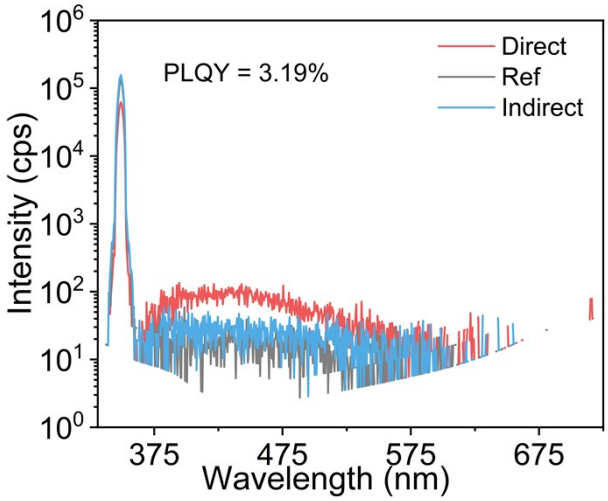


**Figure S10.** The PLQY of **1** at 300 K.

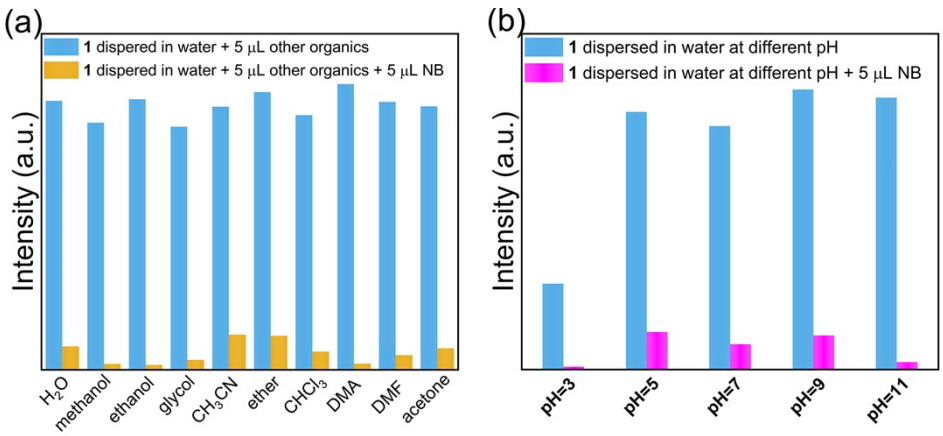


**Figure S11.** (a) Anti-interference study: NB detection unaffected by other organics, (b) pH-dependent selectivity toward NB (pH 3–11).

† These authors contributed equally.

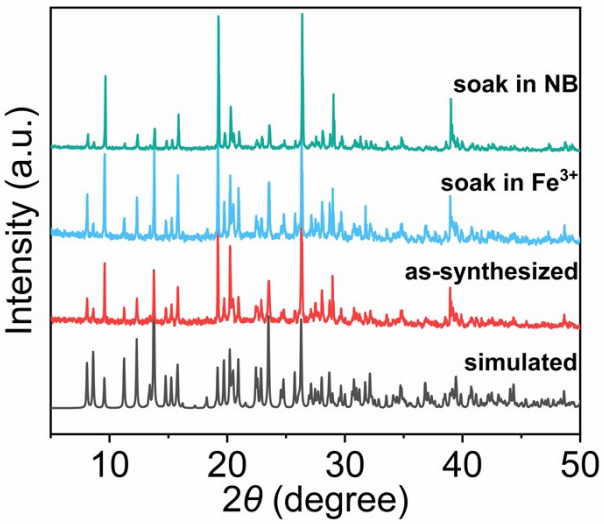


**Figure S12.** PXRD patterns of **1** after soaking in $Fe^{3+}$ ion and NB solution for 24 h.

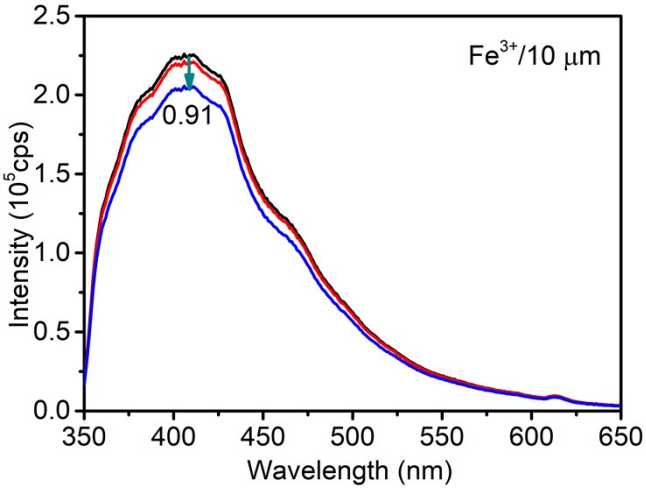


**Figure S13.** Reproducibility and reusability for compound **1** in $Fe^{3+}$ sensing at 10 μM.

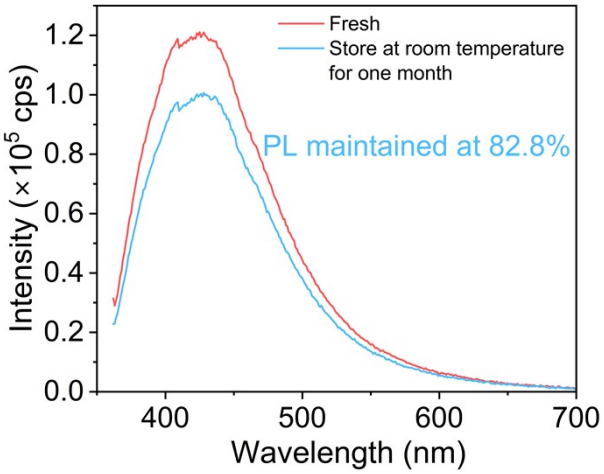


**Figure S14.** Fluorescence emission spectra of compound **1** before and after storage at room temperature for one month.

† These authors contributed equally.

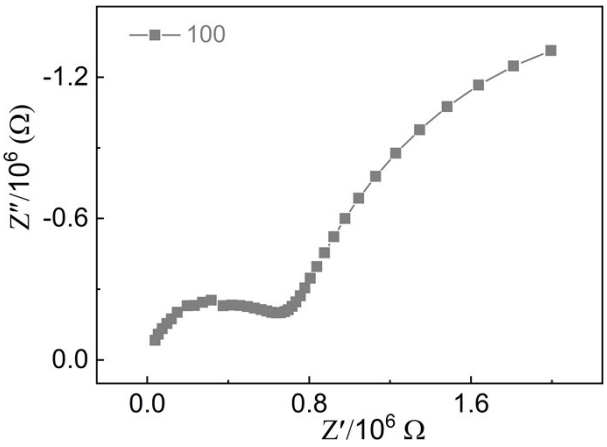


**Figure S15.** Nyquist plots at 25 °C under 100% RH.

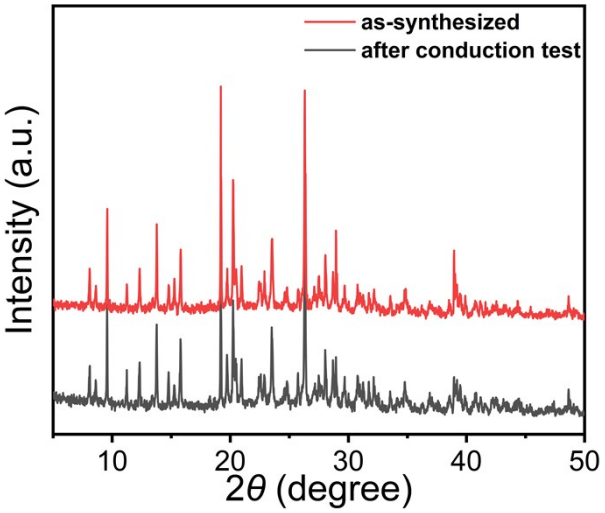


**Figure S16.** PXRD patterns of **1** after proton conduction test at 75 ºC and 100% RH for 8 h.

**Table S1.** XRD Crystallographic Data for **1**

| | |
|---|---|
| CCDC | 2523636 |
| Formula | $C_{18}H_{16}O_{11.5}N_3Ba$ |
| $F_w$ | 579.54 |
| Temperature/K | 299.83(10) |
| Crystal system | Monoclinic |
| Space group | *I*2/a |
| *a*/Å | 18.6600(5) |
| *b*/Å | 13.5527(4) |

† These authors contributed equally.

| | |
|---|---|
| $c$/Å | 15.8810(4) |
| $\alpha$/° | 90 |
| $\beta$/° | 97.631(2) |
| $\gamma$/° | 90 |
| $V$/Å$^3$ | 3980.63(19) |
| $Z$ | 8 |
| $\rho_{calc}$ g/cm$^3$ | 1.9339 |
| $\mu$/mm$^{-1}$ | 2.068 |
| $F$(000) | 2216.2 |
| Reflections collected | 16485 |
| Independent reflections | 4438 |
| Data/restraints/parameters | 4438/0/304 |
| $\theta$ range (deg) | 3.72 to 58.62 |
| $R^1$ [$I >= 2\sigma(I)$] | 0.0410 |
| w$R^2$ [all data] | 0.1288 |
| GOF on $F^2$ | 1.017 |
| $\rho_{max}/\rho_{min}$, e Å$^{-3}$ | 1.87/–1.37 |

$^a R_1 = ||F_o| - |F_c||/|F_o|$. $^b wR_2 = [w(F_o^2 - F_c^2)^2]/[w(F_o^2)^2]^{1/2}$.

**Table S2.** Selected lengths (Å) and angles (º) for the as-synthesized crystals of **1**.

| Atom–Atom | Length/Å |
|---|---|
| Ba2–Ba1$^1$ | 4.7129(4) |
| Ba2–O3$^1$ | 2.813(2) |
| Ba2–O3$^2$ | 2.813(2) |
| Ba2–O8 | 2.680(2) |
| Ba2–O8$^3$ | 2.680(2) |
| Ba2–O2W | 2.741(3) |
| Ba2–O2W$^3$ | 2.741(3) |
| Ba2–O1W$^3$ | 2.749(4) |

† These authors contributed equally.

| | |
|---|---|
| Ba2–O1W | 2.749(4) |
| Ba1–O3 | 2.822(2) |
| Ba1–O3$^{4}$ | 2.822(2) |
| Ba1–O6$^{5}$ | 2.822(3) |
| Ba1–O6$^{6}$ | 2.822(3) |
| Ba1–O2$^{7}$ | 2.876(3) |
| Ba1–O2$^{8}$ | 2.876(3) |
| Ba1–O5$^{5}$ | 3.072(3) |
| Ba1–O5$^{6}$ | 3.072(3) |
| Ba1–O3W | 2.674(5) |

| Atom–Atom–Atom | Angle/° |
|---|---|
| O5$^{7}$–Ba1–O5$^{8}$ | 151.73(15) |
| O3$^{2}$–Ba2–O3$^{1}$ | 66.59(10) |
| O3W–Ba1–O3$^{4}$ | 146.83(5) |
| O3W–Ba1–O3 | 146.82(5) |
| O3W–Ba1–O6$^{8}$ | 72.91(7) |
| O3W–Ba1–O6$^{7}$ | 72.91(7) |
| O3W–Ba1–O2$^{6}$ | 85.82(8) |
| O83–Ba2–O3$^{2}$ | 74.82(9) |
| O8–Ba2–O31 | 74.82(9) |
| O83–Ba2–O3$^{1}$ | 139.93(9) |
| O8–Ba2–O3$^{2}$ | 139.93(9) |
| O8–Ba2–O8$^{3}$ | 144.95(15) |
| O8–Ba2–O2W | 99.11(9) |
| O8–Ba2–O2W3 | 89.38(9) |
| O83–Ba2–O2W3 | 99.11(9) |
| O83–Ba2–O2W | 89.38(9) |

† These authors contributed equally.

| | |
|---|---|
| O83–Ba2–O1W | 85.17(13) |
| O83–Ba2–O1W3 | 66.14(14) |
| O8–Ba2–O1W3 | 85.17(13) |
| O8–Ba2–O1W | 66.14(14) |
| O3W–Ba1–O2[5] | 85.82(8) |
| O3W–Ba1–O5[7] | 75.86(7) |
| O3W–Ba1–O5[8] | 75.86(7) |
| O2W–Ba2–O3[2] | 81.37(9) |
| O2W–Ba2–O3[1] | 74.96(9) |
| O2W[3]–Ba2–O3[2] | 74.96(9) |
| O2W[3]–Ba2–O3[1] | 81.37(9) |
| O2W[3]–Ba2–O2W | 151.65(15) |
| O2W–Ba2–O1W | 70.95(16) |
| O2W–Ba2–O1W3 | 136.38(16) |
| O2W[3]–Ba2–O1W | 136.38(16) |
| O2W[3]–Ba2–O1W3 | 70.95(16) |
| O1W–Ba2–O3[1] | 121.91(11) |
| O1W–Ba2–O3[2] | 145.93(15) |
| O1W[3]–Ba2–O3[2] | 121.91(11) |
| O1W[3]–Ba2–O3[1] | 145.93(15) |

**Symmetry codes for 1:** [1] *x*, 1/2 – *y*, 1/2 + *z*; [2] 1/2 – *x*, 1/2 – *y*, 1/2 – *z*; [3] 1/2 – *x*, *y*, 1 – *z*; [4] 1/2 – *x*, *y*, – *z*; [5] 1 – *x* , 1 – *y*, –*z*; [6] –1/2 + *x*, 1 – *y*, *z*; [7] 1 – *x* , 1 – *y*, 1 – *z*; [8] –1/2 + *x*,1–*y*, –1+ *z*.

**Table S3.** The geometrical parameters of π–π interactions between aromatic rings in **1** calculated by the PLATON software.

| Cg(I)–Cg(J) | Cg–Cg(Å) | *α*(°) | *β*(°) | *γ*(°) | CgI_Perp(Å) | CgJ_Perp(Å) | Slippage(Å) |
|---|---|---|---|---|---|---|---|
| Cg1–Cg3 | 3.7504(17) | 1.83(14) | 25.2 | 26.8 | 3.3476(11) | 3.3936(12) | 1.597 |
| Cg2–Cg3 | 3.6340(17) | 4.76(14) | 16.0 | 19.8 | 3.4202(11) | 3.4930(12) | 1.002 |

† These authors contributed equally.

| | | | | | | | |
|---|---|---|---|---|---|---|---|
| Cg3–Cg2 | 3.7505(17) | 1.83(14) | 26.8 | 25.2 | 3.3935(12) | 3.3477(11) | 1.691 |
| Cg3–Cg2 | 3.6340(17) | 4.76(14) | 19.8 | 16.0 | 3.4930(12) | 3.4201(11) | 1.228 |

**Table S4.** Hydrogen bonds information within **1**.

| D–H | A | *d*(D–H) (Å) | *d*(H…A) (Å) | *d*(D…A) (Å) | ∠DHA |
|---|---|---|---|---|---|
| O1–H1 | O6 | 0.82 | 1.70 | 2.516(4) | 170 |
| O2W–H2WA | O7 | 0.85 | 1.99 | 2.833(4) | 168 |
| N1–H1A | O4W | 0.86 | 1.95 | 2.737(6) | 152 |
| N1–H1A | O4X | 0.86 | 1.95 | 2.789(12) | 166 |
| O2W-H2WB | N3 | 0.85 | 2.24 | 3.032(4) | 155 |
| O3W-H3WA | N2 | 0.85 | 2.05 | 2.892(4) | 173 |
| O3W-H3WB | N2 | 0.85 | 2.13 | 2.982(4) | 150 |
| O1W-H1WA | N2 | 0.85 | 2.54 | 2.926(6) | 109 |
| O1W-H1WB | O4 | 0.85 | 2.35 | 3.184(5) | 165 |
| O7-H7 | O4 | 0.82(3) | 1.68(3) | 2.493(4) | 174(9) |
| O4W-H4WA | O5 | 0.85 | 1.90 | 2.675(6) | 151 |
| O4W-H4WB | O5 | 0.85 | 2.32 | 3.135(10) | 160 |

**Table S5.** Summary of SHAPE analysis for **1**

| Metal | label | shape | symmetry | Distortion(τ) |
|---|---|---|---|---|
| Ba1 | EP-9 | Enneagon | $D_{9h}$ | 31.555 |
| | OPY-9 | Octagonal pyramid | $C_{8v}$ | 24.906 |
| | HBPY-9 | Heptagonal bipyramid | $D_{7h}$ | 13.891 |
| | JTC-9 | Johnson triangular cupola J3 | $C_{3v}$ | 13.340 |
| | JCCU-9 | Capped cube J8 | $C_{4v}$ | 8.099 |

† These authors contributed equally.

| | | | | |
|---|---|---|---|---|
| | **CCU-9** | **Spherical-relaxed capped cube** | **$C_{4v}$** | **7.225** |
| | JCSAPR-9 | Capped square antiprism J10 | $C_{4v}$ | 11.555 |
| | CSAPR-9 | Spherical capped square antiprism | $C_{4v}$ | 10.874 |
| | JTCTPR-9 | Tricapped trigonal prism J51 | $D_{3h}$ | 11.279 |
| Ba2 | OP-8 | Octagon | $D_{8h}$ | 31.752 |
| | HPY-8 | Heptagonal pyramid | $C_{7v}$ | 23.098 |
| | HBPY-8 | Hexagonal bipyramid | $D_{6h}$ | 12.642 |
| | CU-8 | Cube | $O_h$ | 9.181 |
| | SAPR-8 | Square antiprism | $D_{4d}$ | 1.763 |
| | **TDD-8** | **Triangular dodecahedron** | **$D_{2d}$** | **1.731** |
| | JGBF-8 | Johnson gyrobifastigium J26 | $D_{2d}$ | 11.874 |
| | JETBPY-8 | Johnson elongated triangular bipyramid J14 | $D_{3h}$ | 28.455 |

**Table S6.** Single crystal data for crystals immersed in solutions of different pH values.

| | a | B | c | *α* | *B* | *Γ* |
|---|---|---|---|---|---|---|
| **1** | 18.660 | 13.5527 | 15.881 | 90 | 97.63 | 90 |
| pH=3 | 18.646 | 13.531 | 15.874 | 90 | 97.65 | 90 |
| pH=5 | 18.659 | 13.557 | 15.894 | 90 | 97.56 | 90 |
| pH=7 | 18.718 | 13.592 | 15.937 | 90 | 97.62 | 90 |
| pH=9 | 18.652 | 13.551 | 15.874 | 90 | 97.57 | 90 |
| pH=11 | 18.618 | 13.512 | 15.871 | 90 | 97.60 | 90 |

**Table S7.** Literature comparison of fluorescence quenching sensitivity ($K_{SV}$) and proton conductivity ($\sigma$).

† These authors contributed equally.

| Materials (year) | $K_{SV}$/ $M^{-1}$ | Proton conductivity σ/S·cm$^{-1}$ (conditions) | *E*a (eV) | Key notes / comparison focus | Ref |
|---|---|---|---|---|---|
| {[Ba(H$_2$L)(H$_2$O)$_{2.5}$]·H$_2$O}$_n$ (Ba-CP) | $Fe^{3+}$: 3.39×10$^3$; Nitrobenzene: 1.18×10$^3$ | 1.99×10$^{-4}$ (75 °C, 100% RH) | 0.36 | dual function ($Fe^{3+}$ + NB sensing + measurable σ). Most literature reports either sensing or proton transport only. | This work |
| [Dy(spasds)(H$_2$O)$_2$]$_n$ (Dy-CP, 2024) | $Fe^{3+}$: 4.84×10$^4$ | — | — | Much higher $Fe^{3+}$ $K_{SV}$, but no proton-transport data reported (cannot benchmark multifunctionality). | S1 |
| [ZnL(dpa)]n (Zn-CP, 2024) | $Fe^{3+}$: 3.09×10$^4$ | — | — | High $Fe^{3+}$ KSV (10$^4$ level); quenching attributed largely to competitive absorption/coordination; no σ reported. | S2 |
| TbCu-1 heterometallic MOF (2026) | Nitrobenzene: 9.47×10$^3$ | — | — | Good NB sensitivity (10$^3$–10$^4$); focuses on guest-dependent luminescence; no σ reported. | S3 |
| MOF-Ba (alkaline-earth MOF, 2024) | — | 1.28×10$^{-3}$ (65 °C, 98% RH) | — | σ is higher than this work, but fluorescence sensing was not a target/claimed; illustrates that boosting σ often comes without sensing functionality. | S4 |
| Sulfonate CPs / MMMs | — | 1.34×10$^{-3}$ (80 | — | Representative recent | S5 |

† These authors contributed equally.

| Materials (year) | $K_{SV}$/ $M^{-1}$ | Proton conductivity σ/S·cm$^{-1}$ (conditions) | *E*a (eV) | Key notes / comparison focus | Ref |
|---|---|---|---|---|---|
| (2024) | | °C, 95% RH, MMM based on Cu-SAT); $0.91\times10^{-3}$ (80 °C, 95% RH, Ca-NDS(water)-MMM) | | CP/MOF proton conductors; emphasize that state-of-the-art σ is usually achieved in membranes; sensing metrics are not provided. | |
| Ni-BAND hydrogen-bonded CP thin film (2025) | — | 0.09 (room temperature, RH > 90%) | — | Exceptional σ at room temperature (thin film) for mixed protonic–electronic conductor; far from typical luminescent-sensor design space. | S6 |

Note: "—" indicates the corresponding value was not reported in the cited work.

**Table S8.** The proton conductivity of **1** at variable temperatures under 100% RH.

| *T*/°C | $\sigma$ / S·cm$^{-1}$ |
|---|---|
| 25 | $3.08\times10^{-5}$ |
| 35 | $4.96\times10^{-5}$ |
| 45 | $7.54\times10^{-5}$ |
| 65 | $1.46\times10^{-4}$ |
| 75 | $1.99\times10^{-4}$ |

**References**

† These authors contributed equally.

S1. Y. Wang, B. An, S. Li, L. Chen, L. Tao, T. Fang and L. Guan, *Molecules*, 2024, **29**, 4495.

S2. B. Zhao, J. Lu, H. Liu, S. Li, Q. Sun and B. Zhang, *CrystEngComm*, 2024, **26**, 1319–1327.

S3. G.-L. Zhu, A.-N. Dou, S. Yin, L.-B. Yang, W.-H. Mu, R.-R. Zhu and A.-X. Zhu, *Dyes Pigments*, 2026, **245**, 113252.

S4. G. Luo, S. Zhang, S.-L. Zhang, D. Zhou, C. Huang, D. Chen, B. Zhu, J. Yang and L. Shen, *J. Mol. Struct*., 2024, **1299**, 137145.

S5. C. Sun, C. M. Pask, S. T. Pham, E. Rapaccioli, A. J. Britton, S. Micklethwaite, A. Bell, M. O. Besenhard, R. Drummond-Brydson, K.-J. Wu and S. M. Collins, *J. Mater. Chem. A*, 2024, **12**, 18440–18451.

S6. M. Park, H. Ju, J. Oh, K. Park, H. Lim, S. M. Yoon, I. Song, *Nat. Commun*., 2025, **16**, 1316.

† These authors contributed equally.